Voltage-gated membrane currents in neurons involved in odor information processing in snail procerebrum

Z. Pirger, I. Battonyai, N. Krajcs, K. Elekes & T. Kiss

Brain Structure and Function

ISSN 1863-2653

Brain Struct Funct
DOI 10.1007/s00429-013-0526-6

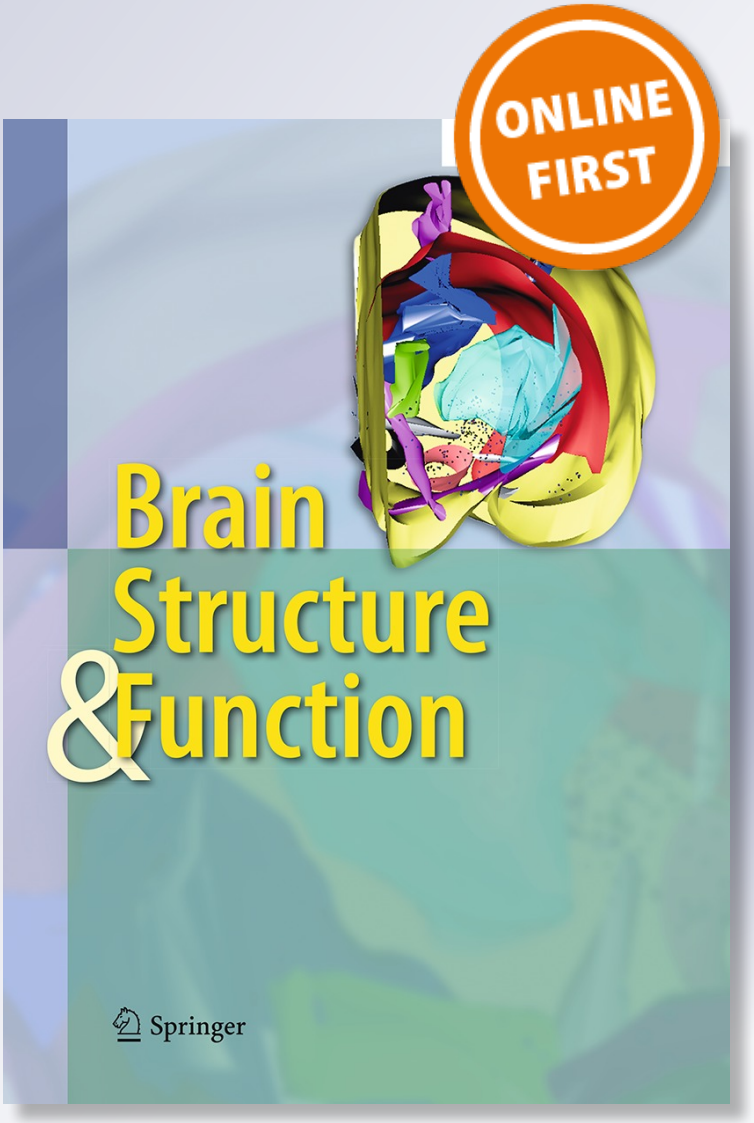

Springer

Brain Struct Funct
DOI 10.1007/s00429-013-0526-6

ORIGINAL ARTICLE

Voltage-gated membrane currents in neurons involved in odor information processing in snail procerebrum

Z. Pirger · I. Battonyai · N. Krajcs · K. Elekes · T. Kiss

Received: 19 November 2012 / Accepted: 8 February 2013

Abstract The procerebrum (PC) of the snail brain is a critical region for odor discrimination and odor learning. The morphological organization and physiological function of the PC has been intensively investigated in several gastropod species; however, the presence and distribution of ion channels in bursting and non-bursting cells has not yet been described. Therefore, the aim of our study was to identify the different ion channels present in PC neurons. Based on whole cell patch-clamp and immunohistochemical experiments, we show that Na^+-, Ca^{2+}-, and K^+-dependent voltage-gated channels are differentially localized and expressed in the cells of the PC. Different Na-channel subtypes are present in large (10–15 μm) and small (5–8 μm) diameter neurons, which are thought to correspond to the bursting and non-bursting cells, respectively. Here, we show that the bursting neurons possess fast sodium current (I_{NaT}) and $Na_V1.9$-like channels and the non-bursting neurons possess slow sodium current (I_{NaT}) and $Na_V1.8$-like channels in addition to the L-type Ca^-, $K_V4.3$ (A-type K-channel) and $K_V2.1$ channels. We suggest that the bursting and/or non-bursting character of the PC neurons is at least partly determined by the battery of ion-channels present and their cellular and subcellular compartmentalization.

Keywords Snail · Olfaction · Ion currents · Procerebrum

Z. Pirger · I. Battonyai · N. Krajcs · K. Elekes · T. Kiss (✉)
Department of Experimental Zoology, Balaton Limnological Institute, Centre for Ecological Research, Hungarian Academy of Sciences, Klebelsberg Kuno Str. 3, 8237 Tihany, Hungary
e-mail: kiss.tibor@okologia.mta.hu

Z. Pirger
School of Life Sciences, University of Sussex, Falmer, Brighton BN1 9QG, UK

Introduction

In gastropods, data from a number of studies indicate a key role of the procerebrum (PC) in central olfactory information processing. The existence of the PC can be considered to be the result of an evolutionary process during the successful adaptation of snails and slugs to a terrestrial environment, where olfaction is pivotal to obtain information for foraging and reproduction (Ache and Young 2005; Chase 2000, 2002; Gelperin 1999). The organization of the olfactory system is remarkably similar in different invertebrates and vertebrates, suggesting that this type of sensory modality relies on well-conserved principles (Hildebrand and Shepherd 1997). Anatomically the PC displays similarities with the olfactory bulb of vertebrates meanwhile its architecture differs from the rest of the gastropod brain (Bullock and Horridge Bullock and Horridge 1965; Chase 2000; Chase and Tolloczko 1993). The PC can morphologically be divided into three parts: the cell body layer, the terminal and neuropil and the internal neuropil (Chase 2002; Zaitseva 2000; Zs.-Nagy and Sakharov 1970). The cell body layer consists of a high number of densely packed 5- to 8-μm diameter neurons, which profoundly outnumber the cells found in the rest of the central nervous system (CNS). The neuropils contain axon processes of both intrinsic and extrinsic origin and are the major site of synaptic connections (Ratté and Chase 2000; Watanabe et al. 1998). The odor signals from the tip of the superior tentacles are carried by the olfactory nerve to the neurons of the PC. It has been observed that processes of several olfactory receptor neurons establish synaptic contacts at the level of the tentacle ganglion (TG), which is the first relay site; meanwhile other contacts directly reach the PC or project outside the PC (Chase and Tolloczko 1993; Ratté and Chase 2000). PC neurons display a resting cyclic electrical activity of 0.7 Hz, which is important for the

Published online: 27 February 2013

storage of odor memory and odor discrimination (Balaban and Maksimova 1993; Delaney et al. 1994; Gelperin and Tank 1990; Schütt et al. 2000). This oscillatory activity was shown to be modulated by odor stimuli (Delaney et al. 1994; Gelperin and Tank 1990; Gervais et al. 1996; Kimura et al. 1998; Kleinfeld et al. 1994) and by signal molecules such as nitrogen and carbon monoxide, γ-aminobutyric acid, 5-hydroxytryptamine (5-HT), dopamine (DA), glutamate (Glu), acetylcholine (ACh) and endogenous neuropeptides such as FMRFa and catch-relaxing peptide, which are present in the PC (Battonyai and Elekes 2012; Cooke and Gelperin 1988; Elekes and Nassel 1990; Gelperin et al. 1993, 2000; Hernadi et al. 1995; Inoue et al. 2001; Kobayashi et al. 2010). It was observed that 5-HT and DA excited PC neurons and promoted transitions from steady to bursting activity. Both amines elicited increases in intracellular Ca^{2+} level concomitant with the increase in action potential (AP) frequency. Glu suppressed AP firing and reduced intracellular Ca^{2+} (Rhines et al. 1993a). Perforated patch recording studies have affirmed the existence of two types of neurons with different spontaneous electrical activity in the PC of *Limax maximus*: bursting and non-bursting neurons, which are modulated differentially by ACh (Kleinfeld et al. 1994; Watanabe et al. 1998). Data obtained by concurrent optical and intracellular recordings led to the suggestion that Ca^{2+} is the major carrier for the inward current during APs of bursting neurons (Wang et al. 2001). The bursting cells are regarded as local inhibitory interneurons and their axons are located in the cell body layer of the PC (Ratté and Chase 2000). In contrast, the non-bursting cells project extensively branching processes to the neuropil layer, where they establish synaptic contacts with extrinsic neurons (Ratte and Chase 1997; Watanabe et al. 1998).

The morphology and electrophysiology of single PC neurons have already been investigated in several gastropod species. However, the relationship between the electrophysiological properties of bursting and non-bursting cells and their ion channel characteristics has not yet been described. A detailed knowledge of the properties of voltage-gated ion channels expressed by neurons would contribute greatly to our understanding of how the activity of these neurons underlies odor processing. Therefore, the aim of the present study is to identify which types of ion channels are present in PC neurons using voltage-clamp technique to record membrane currents and supporting these results using immunohistochemistry.

Materials and methods

Experimental animals and preparation

Measurements were performed on adult specimens of the terrestrial snail *Helix pomatia* L., collected locally. The snails were kept under humid conditions (93–98 %) in a terrarium at room temperature (20 ± 2 °C) and fed twice a week on lettuce. The CNS was dissected and pinned out in a Sylgard-lined chamber containing snail saline composed of (in mM): 80 NaCl, 4 KCl, 10 $CaCl_2$, 5 $MgCl_2$, 10 Tris–HCl, pH 7.4. The thick connective tissue sheath was removed from the cerebral ganglia (CG) and then the perineurium was softened by 1 % protease treatment (Sigma XIV, Sigma) for 5–8 min. Thereafter, both PC lobes were separated from the rest of the CG. The PC cells were mechanically isolated by sucking them repeatedly into glass pipettes of a decreasing tip diameter. The dissociated PC cells were left for 10 min to adhere to the bottom of the recording chamber pretreated with polylysine. Experiments were carried out on freshly isolated neurons. The recording chamber was perfused continuously with snail saline using a gravity feed system and the superfluous solution was removed by suction. All experiments were performed at room temperature in accordance with the Hungarian Council of Animal Care guidelines on the ethical use of animals.

Recording methods

Current recording was performed under an inverted microscope (Leitz Labovert FS, Germany) using tight seal whole cell patch-clamp recording. In several experiments, instead of rupturing the cell membrane by additional suction, the nystatin (100 μg/ml) method was used to permeabilize the cell membrane in the patch pipette. No differences were detected between the currents recorded using these two methods. An EPC-7 patch-clamp amplifier (List Electronics, Darmstadt, Germany) was used to monitor voltage-gated currents. Most of the data were obtained from spherical cells with diameter of 5–8 μm. Occasionally, bipolar ellipsoid cells with diameters of 10–15 μm were also used. Microelectrodes were pulled from borosilicate glass pipettes (PG150-T-7.5, Harvard Apparatus, Edenbridge, UK) and fire-polished to a 6–7 MΩ tip resistance when filled with pipette solution containing (in mM): 140 KCl, 1.2 $MgCl_2$, 0.1 $CaCl_2$, 10 HEPES, 10 glucose, pH 7.2 adjusted with NaOH. Series resistance compensation at the 60 % level was used for most recordings. For data acquisition and clamp protocols, the amplifiers were connected via a TL DMA interface (Axon Instruments, Union City,CA, USA) to a computer supplied with pClamp 5.5 software (Axon Instruments, Union City, CA, USA). Signals were sampled at 20 kHz and stored digitally for offline analysis, and a leak-subtraction protocol was used during acquisition. Currents were separated using special voltage protocols, as in the case of the transient K^+-current, or by applying special dissecting solutions, used to study inward Ca^{2+}- and Na^+-currents or outward K^+-currents.

In voltage-clamp experiments, the Ca^{2+}-currents were isolated by substituting external Na^+ with NMDG and blocking outward currents by adding 30 mM TEA and 4 mM 4-AP; Na^+-currents were recorded in a solution containing (in mM): 90 NaCl, 4 KCl, 1 $CaCl_2$; 5 $MgCl_2$, 10 Tris–HCl; 30 TEA; 4 4-AP and 50 µM $CdCl_2$, pH7.4. Outward currents were recorded in Na^+-free solution substituted with NMDG. Current traces were subjected to a low-pass Gaussian filter (1 kHz) and analysis was performed using Axon pClamp 5.5 or OriginLab Corporation, Origin8.5 software. Data are presented as mean ± SE. Comparisons were considered significant when $P < 0.05$.

Immunohistochemistry (IHC)

The CGs of *Helix pomatia*, including PCs, were fixed with 4 % paraformaldehyde diluted in 0.1 M phosphate buffer (PB; pH 7.4) overnight at 4 °C. 14–16 cryostat sections were placed on chrome-alum gelatin coated slides and processed for IHC as follows. (1) Incubation for 30 min at room temperature in PB saline containing 0.25 % TX-100 (PBS-TX), 0.25 % bovine serum albumin (BSA) and 4 % normal goat serum (PBS-TX-BSA-NGS) to block non-specific binding sites. (2) Incubation with the following primary antibodies (Abs): polyclonal rat $Na_V\beta2$, $Na_V1.9$, $Na_V1.8$, $K_V4.3$ (Alomone Laboratory, Jerusalem, Israel; 1:200 or 1:1,000), and monoclonal mouse $K_V2.1$ Ab (Neuromab/Antibodies Incorporated, Davis, CA, USA, 1:500) diluted in PBS-TX-BSA. (3.1) Incubation of sections reacted to $Na_V1.8$ Ab with polyclonal swine anti-rabbit (Dako; diluted 1:40). (3.2) Incubation of sections reacted to $K_V4.3$ Ab with rabbit anti-donkey IgG conjugated with TRITC or FITC (Dako; 1:200). All Ab incubations were performed overnight at 4 °C. (3.3) Incubation of sections reacted to $K_V2.1$ Ab for 5 h at room temperature with biotin-conjugated goat anti-mouse IgG (1:200) followed by avidin-HRP (1:200) (both from vector Laboratory, Burlingame, CA, USA); labeling for 1 h at room temperature. The reaction was visualized in Tris–HCl buffer (pH 7.4) by adding 0.05 % 3′3-diaminobenzidine (DAB, Sigma, St.Louis, Missouri, MO, USA) as chromogen and 0.01 % H_2O_2 as substrate. The sections mounted in a 1:1 mixture of glycerin-PBS were viewed with a Zeiss Axioplan compound microscope attached to a CCD camera (Alpha DCM510, Hangzhou Scopetek Opto-Electric, Hangzhou, China).

Two types of control experiments were performed. In a specificity preadsorption test, the diluted Abs were mixed and blocked with their antigen peptides (Alomone Laboratory, 1 µg peptide/1 µg Ab) overnight at 4 °C. As a method control, the primary Ab was either omitted or substituted with BSA. No immunostaining could be observed following these control experiments.

Results

Excitability of isolated cells

A typical view of dissociated PC neurons is shown in Fig. 1a. The neurons show mostly a spherical shape and truncated processes and were typically 5–8 µm in diameter. Occasionally, slightly elongated bipolar cells with a 10- to 15-µm diameter were also observed (Fig. 1b), suggesting that the PC cell population was not morphologically homogenous. In current clamp mode, the resting membrane potential (RMP) was measured between –42 and –67 mV. For 46 tested cells, the mean RMP was –50 ± 8 mV measured in physiological solution. The distribution of the RMP was homogeneous suggesting that functional discrimination based on the RMP between the dissociated cells was not possible. Spontaneous action potentials (AP) were never observed contradicting observations obtained in cultured PC neurons and in an in vivo preparation of *Limax* (Rhines et al. 1993a; Watanabe et al. 1998). Voltage-clamping of the isolated PC cells in physiological solution revealed the presence of a complex current wave form comprising inward and outward components (Fig. 1c, d). Figure 1c shows a family of current traces with a slowly activating and inactivating inward current and a transient and delayed K^+-currents. Figure 1d shows a cell type that was characterized by the presence of a fast activating and inactivating inward current and a delayed K^+-current. The different current types recorded at the same holding potential (HP = –60 mV) but not at different HPs (–40 and –60 mV) supported the presence of at least two different populations of neurons.

Inward Ca^{2+}-current

Two types of experiments were performed to record Ca^{2+}-currents (I_{Ca}) in dissociated PC cells: changing the HP, and using a physiological solution of special composition. Whole cell patch-clamp recordings revealed inward currents elicited by depolarizing voltage steps when the HP was held at –40 mV (Fig. 2a). At this potential, the transient inward Na^+-current (I_{NaT}) and I_{Ca} were activated. To isolate inward I_{Ca}, recordings were performed in a solution containing *N*-methyl-D-glucamine (NMDG) instead of Na^+-ions in addition to 30 mM tetraethylammonium chloride (TEA) and 4 mM 4-aminopyridine (4-AP). Fig. 2b shows a family of typical I_{Ca} traces demonstrating a rapid onset and little inactivation during a 40-ms voltage step. Current–voltage (*I–V*) characteristics (Fig. 2c) support the earlier observation that the inward current was carried by high threshold-type Ca-channels: the inward current was first seen when the cell membrane was depolarized to test potentials greater than –20 mV, and the

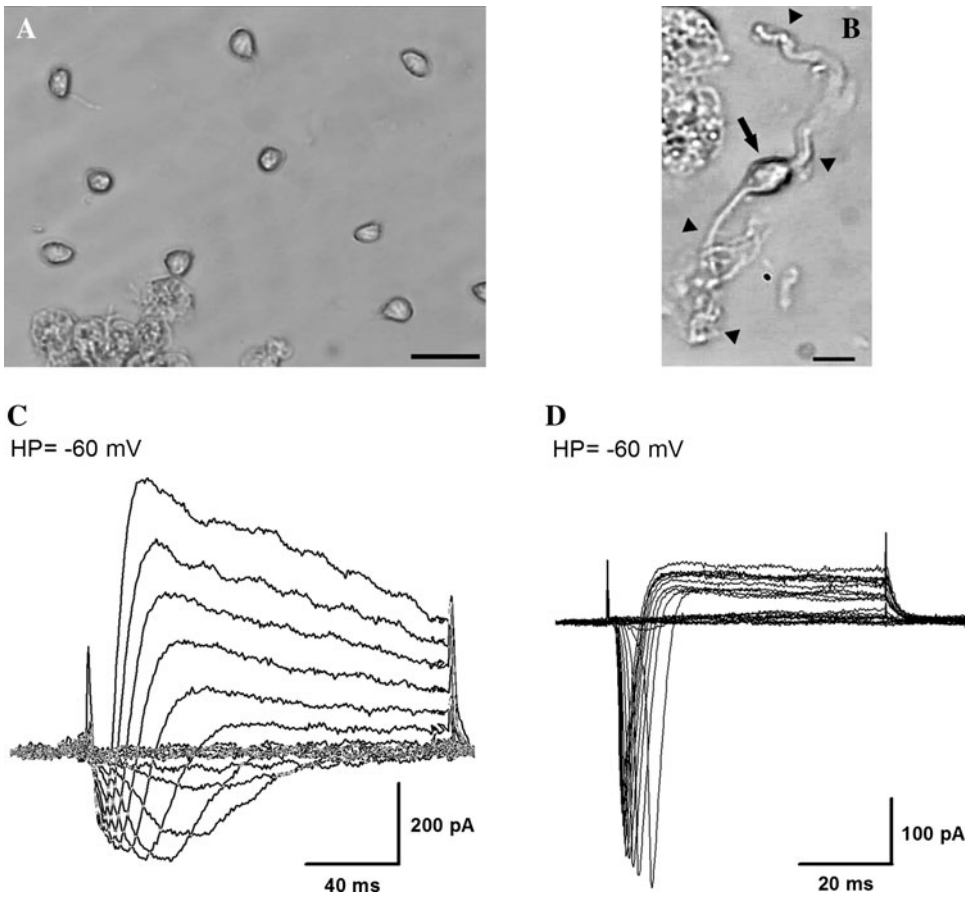

Fig. 1 Membrane currents of isolated PC cells. **a** Dissociated small-diameter (5–8 μm) neurons are attached to the bottom of the recording chamber. **b** An example of a 10- to 15-μm cell with typical bipolar morphology. *Arrows* show neuronal processes. *Horizontal bars* mark 10 μm. **c** Family of current traces elicited by 160-ms test pulses from −60 to +40 mV (5-mV increments). The cell displayed inward, transient, and delayed outward currents in normal physiological solution. **d** Family of current traces recorded from a cell with a fast inward current in normal physiological solution. Current traces were elicited by 60 ms depolarizing test pulses from −60 to +30 mV (5-mV increments)

current activated at –20 mV peaked at +10 mV and reversed at ~+60 mV suggesting that the current was carried by Ca^{2+}-ions. The I_{Ca} was inhibited effectively and reversibly by 50 μM $CdCl_2$.

Inward Na^+-currents

Occasionally, an I_{NaT} was observed in isolated PC cells bathed in physiological solution of normal ion composition. To facilitate isolation of the I_{Na}, experiments were performed in a solution containing 30 mM TEA and 4 mM 4-AP to block outward currents and 50 μM $CdCl_2$ to eliminate the contribution of the inward I_{Ca}. Voltage-clamp recordings of snail PC cells revealed the presence of both persistent (I_{NaP}) and I_{NaT} currents (Fig. 2d). I_{NaP}s were already activated at –55 mV and in several cells, only I_{NaP} was recorded between –60 and –20 mV (Fig. 2e). Two types of I_{NaT} were observed: the fast and slow currents. The fast I_{NaT} was activated and inactivated within 20–25 ms (Fig. 3a) and had average amplitude of 350 ± 38 pA (Fig. 3e). The slow I_{NaT} was activated and inactivated over a period of 25–80 ms (Fig. 3c) and had average amplitude of 195 ± 38 pA (Fig. 3e). The average normalized *I–V* characteristics revealed that the fast I_{NaT} activated at around –45 mV peaked at –5 mV and reversed at around +60 mV (Fig. 3b). The average normalized *I–V* characteristic of the slow I_{NaT} showed that this current was activated at –50 mV, peaked at +10 mV and reversed at around +80 mV (Fig. 3d). In addition to the I_{NaT} currents, an I_{NaP} was also present with two components that had different activation and inactivation parameters (closed circles in Fig. 3b,d) corresponding well to $Na_V1.9$- and $Na_V1.8$-like channel subtypes described previously in the neurons of the *Helix* CNS (Kiss et al. 2012). The average amplitudes of the I_{NaP} components were 61.0 ± 10.5 and 54.7 ± 7.9 pA, respectively. The electrophysiological results suggest that cells of the PC are armored with different sets of Na-channels. To confirm these electrophysiological data, the expression and distribution of voltage-gated Na-channels in the PC were examined using specific antibodies.

The IHC experiments performed with $Na_V1.8$, $Na_V1.9$, and $Na_V\beta2$ Abs revealed that PC cells express different Na_V subtypes (Fig. 4). $Na_V1.8$-like channels are widely distributed throughout the CG (Fig. 4a, a1). Large- and small-diameter neurons and the neuropil are intensively labeled. The cell body layer of the PC, suggested to represent non-bursting cells, was labeled by $Na_V1.8$ Ab, while the neuropil remained immunonegative (Fig. 4a).

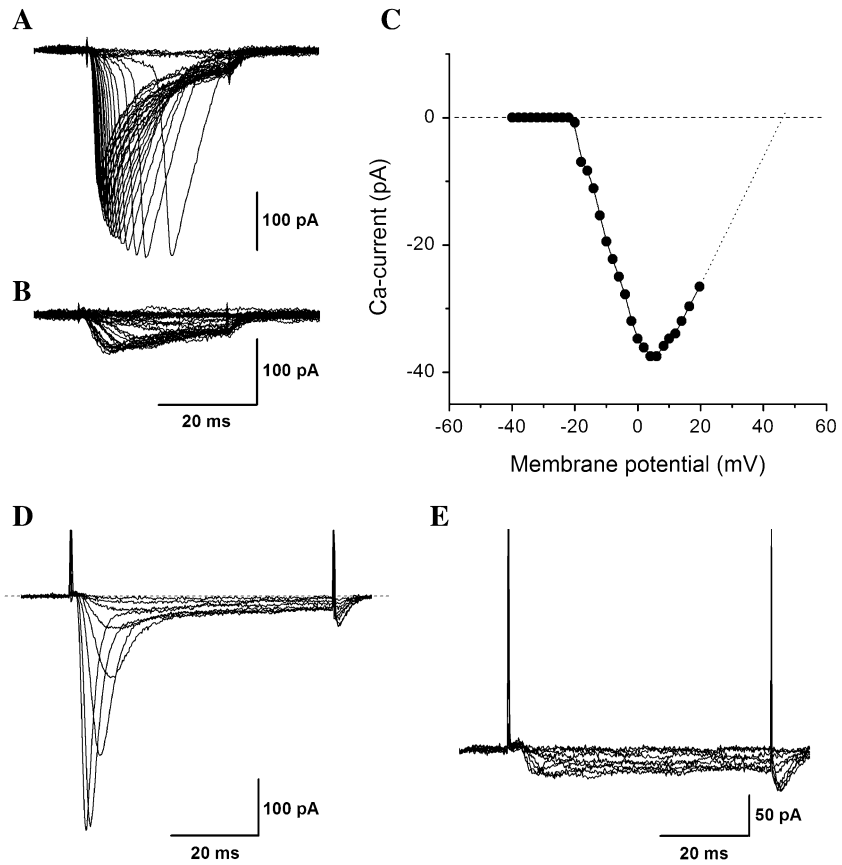

Fig. 2 Voltage-clamp recording of inward I_{Ca} and I_{NaP}. **a** Representative current traces elicited by 30-ms test pulses from a −40 mV HP in a solution containing 30 mM TEA and 4 mM 4-AP. Depolarizing pulses were applied in 2-mV voltage steps to +20 mV. **b** Current traces recorded with the same pulse protocol from the same cell, in a bathing solution where Na^+-ions were replaced by NMDG. **c** The *I–V* characteristic of the inward current recorded in NMDG-solution. **d** The cell was held at an HP of –60 mV and stepped to 0 mV in 2 mV increments. An I_{NaP} component is apparent. **e** In several PC neurons only the I_{NaP} was present. Currents were elicited by 5 mV depolarizing voltage steps from a −60 mV HP to +30 mV

Cells positively labeled with the $Na_V1.9$ Ab were located on the surface of the cell body layer of the PC and at the border between the cellular and neuropil layers (Fig. 4b, b1). These cells were larger in diameter (10–15 µm) than the great majority of PC neurons (5–8 µm) Immunoreactivity of the $Na_V1.9$-like channel was observed in both the soma and neurites; these were identified as bursting cells. Their neurites projected toward the cell body layer of the PC and formed a thin bundle running parallel with the surface, also suggesting that they are interconnected (Fig. 4b). It has been suggested previously that axons of the bursting cells remain within the cell body layer of the PC, where they partly make synaptic contacts with a large number of non-bursting cells (Chase and Tolloczko 1993; Elekes et al. 2012). Figure 4c shows that $Na_V\beta2$ Ab labeled cells and varicosities are widely distributed throughout the CG. Noticeably in the PC, both large- and small-diameter neurons were labeled (Fig. 4c), indicating that the Abs used in our experiment were specific.

Outward K^+-currents (I_K)

Most of the neurons studied here have a variety of K-channels, which are separable by their kinetics, voltage dependence and pharmacology. Under the conditions that isolate outward I_K (low HP or Na^+-free solution), depolarizing impulses evoked outward currents as represented by the current traces shown in Fig. 5a. The outward current began to activate near –30 mV from an HP of –80 mV. The activation rate was voltage dependent, with the current reaching a peak within 5–7 ms with steps to +30 mV. The current was stable and showed little inactivation for depolarizing pulses up to 100-ms durations. In one set of neurons, a slow A-type I_K was observed in addition to the delayed I_K (Fig. 5b). The delayed I_K component, when recorded from an HP of –60 mV was largely attenuated in the presence of 50 mM TEA (Fig. 5c). The *I–V* relationship of the late current measured at the end of 150 ms, and the transient outward current, measured at the peak value, showed that the early current was activated at more negative potentials than the late current and attained higher amplitude (Fig. 5d, e).

IHC experiments revealed a specific expression pattern for the $K_V2.1$ and $K_V4.3$ channels in the *Helix* PC. Both $K_V2.1$ and $K_V4.3$ Ab labeled neurons were found in the cell body layer and their processes were present in the neuropil of the PC. A large number of $K_V2.1$ immunoreactive cells were found throughout the PC cell body layer, forming smaller and larger cell groups (Fig. 6a), while immunoreactivity for $K_V4.3$ channels was confined to smaller units of

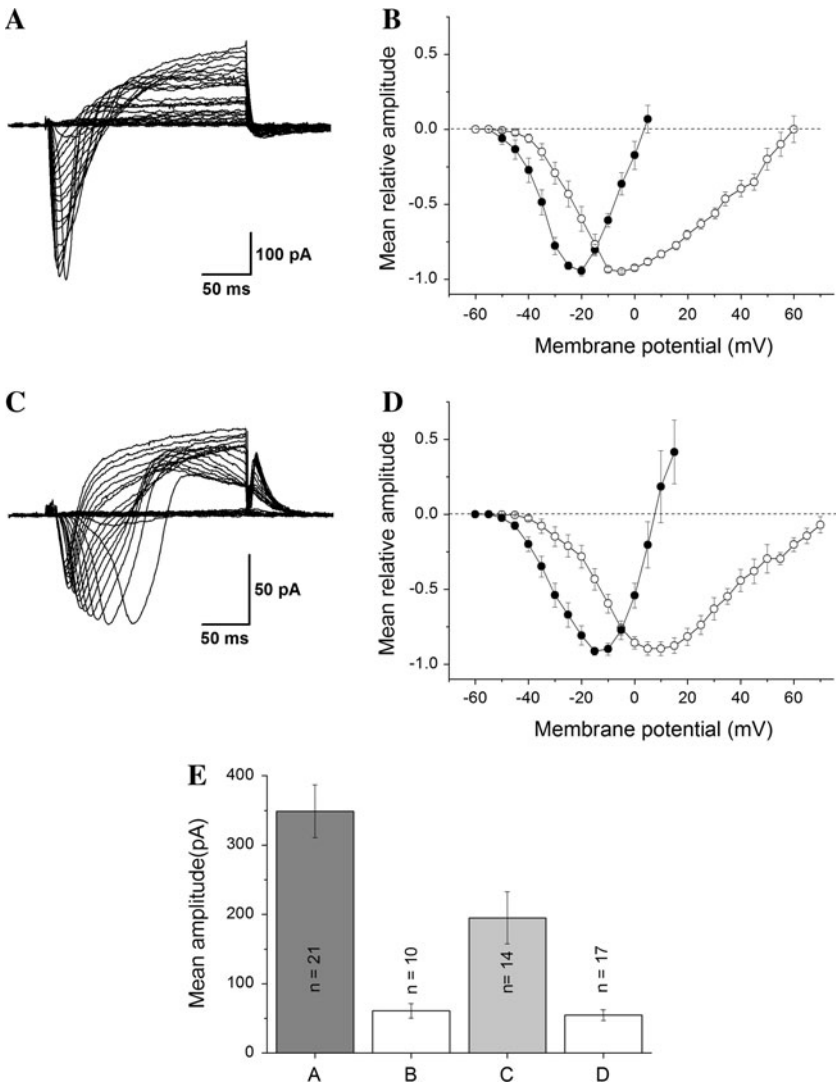

Fig. 3 Voltage-clamp recordings of inward I_{Na} from PC cells. **a** Family of fast I_{NaT}s elicited in 5-mV voltage steps in a solution containing 30 mM TEA, 4 mM 4-AP, 50 µM $CdCl_2$. HP = –60 mV. **b** Mean *I–V* characteristics of an I_{NaP} (*full circles*) and a fast I_{NaT} (*open circles*). **c** Family of slow I_{NaT}s showing different activation kinetics to the cell shown in A. **d** Voltage dependence of the mean peak current amplitudes recorded from cells expressing a slow I_{NaP} (*full circles*) and a slow I_{NaT} (*open circles*). Current amplitudes in **c** and **d** were normalized in each cell measured. **e** Comparison of current amplitudes recorded from the cells expressing fast and slow transient Na^+-currents. The average amplitude of the fast I_{NaT} (*column A*) was two times larger than the average amplitude of the slow I_{NaT} (*column C*). The real amplitudes of the sustained components did not vary from each other (*columns B* and *D*)

small-diameter cells (Fig. 6b). The neuropil region was characterized by varicose fibers intensively labeled for $K_V4.3$ channels, contrary to the overall homogenous appearance of $K_V2.1$ immunolabeling (Fig. 6b). Large size cells did not express transient K-channels although the full complement of K-channels was not examined.

Discussion

Earlier optical and electrophysiological recordings confirmed that the PC contains at least two classes of neurons: bursting and non-bursting neurons (Ermentrout et al. 1998; Kleinfeld et al. 1994; Nikitin et al. 2005). In the PC of *Limax*, bursting and non-bursting cells have been distinguished on the basis of their size, shape, and conduction velocity and it has been suggested that the somata of bursting neurons are larger than those of the non-bursting neurons (Watanabe et al. 1998). Based on electrophysiological and IHC experiments, our data provide for the first time the description and characterization of voltage-dependent membrane currents in the two types of PC neurons of *Helix pomatia* as follows: a delayed and an inactivating outward current, two inward Na-currents, one fast and one slow, two sustained Na^+-currents; a Ca^{2+}-dependent inward current. This set of conductances, along with complex synaptic connections (Elekes et al. 2012), seems to ensure the integrative and odor-coding properties PC cells of gastropod molluscs.

Functional significance of voltage-gated ion-channels in PC neurons

A neuron's activity pattern depends on both intrinsic properties and extrinsic synaptic inputs; how the cell responds to these inputs largely depends on the types and localization of ion channels that are expressed in the cell membrane. Therefore, an understanding of the cellular and subcellular distribution of ion channels in PC neurons and

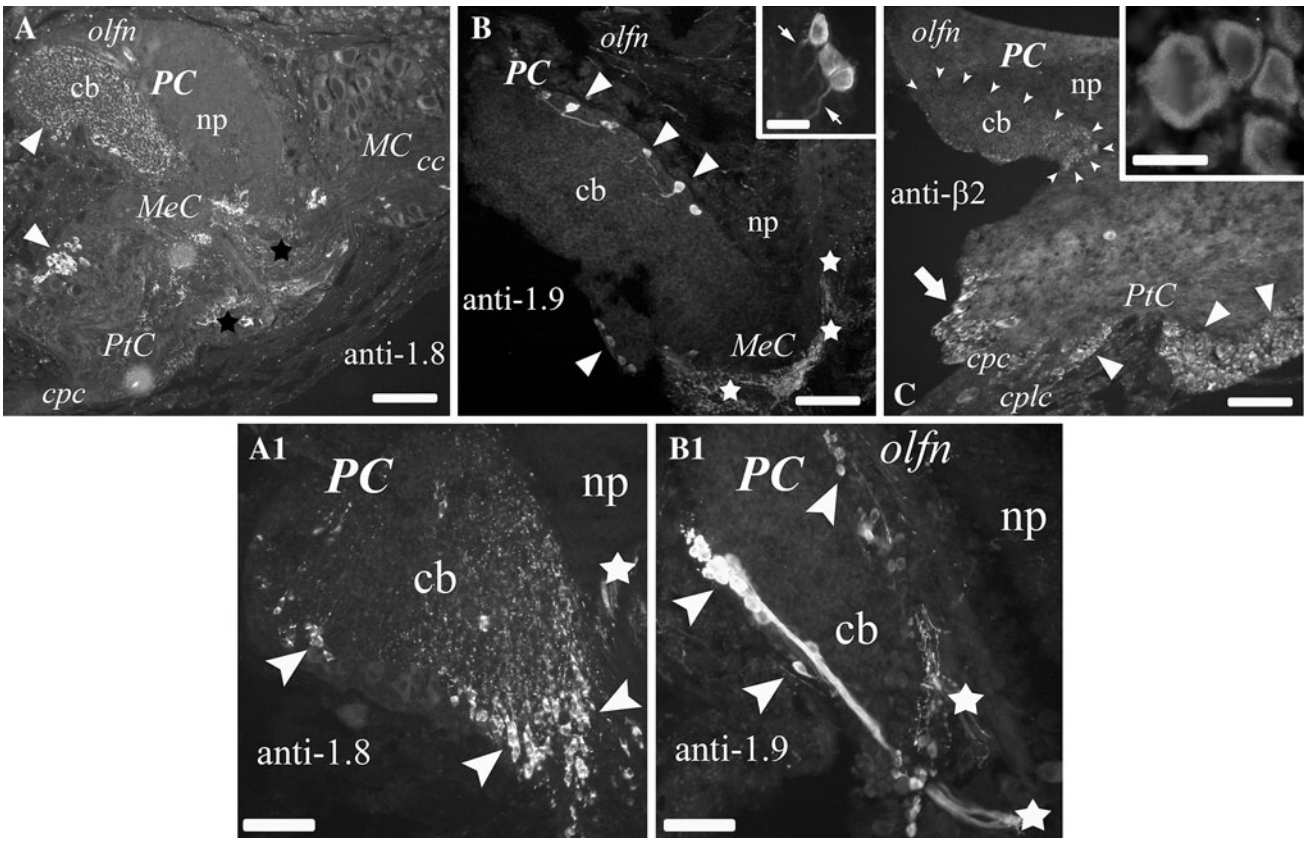

Fig. 4 Distribution of Na-channel expressing neurons in the PC. **a** IHC labeling of the CG with $Na_V1.8$ Ab. *Triangles* mark cell groups and *black stars* mark the neuropil labeled only with $Na_V1.8$ Ab. *a1* Enlarged view of the PC, demonstrating specific labeling of the cell body (cb) layer. **b** $Na_V1.9$ Ab specifically labeled large cells (*triangles*) along the border between the cb and neuropile (np) layers. These cells seem to be horizontally coupled by their axons (*arrows*), which end in the cb layer (*insert*). *b1* Different section plane demonstrating $Na_V1.9$ immunoreactive cells (*arrowheads*) and their axon bundle projecting to the CG (*stars*). **c** The $Na_V\beta2$ subunit is expressed in most of the cells and axons of the CG as revealed by anti-$Na_V\beta2$ Ab. *Small arrowheads* delineate the border between cb and np layers. *Insert* shows the punctate appearance of labeled protein. *PC* procerebrum, *MC* mesocerebrum, *PtC* postcerebrum, *MeC* metacerebrum, *cc* cerebral connective, *olfn* olfactory nerve, *cpc* cerebro-pedal connective, *cplc* cerebro-pleural connective. *Scale bars* **a**, **c** 200 μM; **a1**, **b**, **b1** 50 μm; **b**, **c** *insert* 20 and 30 μm

how each channel subtype contributes to cell excitability is vital for elucidating the underlying mechanism of olfactory information processing. The functional significance of Na-channels with different kinetic parameters has already been described in molluscs (Gilly et al. 1997). The activation kinetic of the fast I_{NaT} in the squid giant axon has a shallow voltage dependence allowing rapid adjustment of the number of open channels. Such activation kinetics is characteristic for axons with fast impulse transmission and provides high safety for excitation. It has been shown that axonal APs in gastropods are largely mediated by Na-channel activity, while the somata of snail neurons are equipped both with Na- and Ca-channels (Gilly et al. 1997). Our experiments on the PC neurons of *Helix* corresponds well to these observations and supports the findings in *Limax*, that APs of the bursting neurons are mediated by I_{Ca} (Wang et al. 2001). In gastropods, however, the rate constant of I_{Na} activation is much more voltage-dependent and is consistent with the slow activation kinetics of Na-channels. This may play a decisive role in integrative and pacemaker properties of neurons as has been proposed for mammals (Llinas 1988). In primary sensory neurons, such as squid olfactory receptor cells, the slowly activating Na-channels ensure spontaneous bursting activity (Chen and Lucero 1999). Although the Na-channels responsible for the fast and slow I_{NaT} were not identified by IHC in this study, we suggest that $Na_V1.1$- and $Na_V1.2$-like channels and L-type Ca-channels are responsible for the initiation and axonal propagation of AP in the PC. We have shown recently that in addition to the $Na_V1.1$- and/or $Na_V1.2$-like channels (Azanza et al. 2008), most of the neurons of the snail brain contain Na $_V1.9$- and/or $Na_V1.8$-like channels (Kiss et al. 2012). In the PC, the presence of two types of neurons was observed expressing $Na_V1.9$-like and $Na_V1.8$-like channels. The expression of the $Na_V1.9$-like subunit correlated with the presence of a

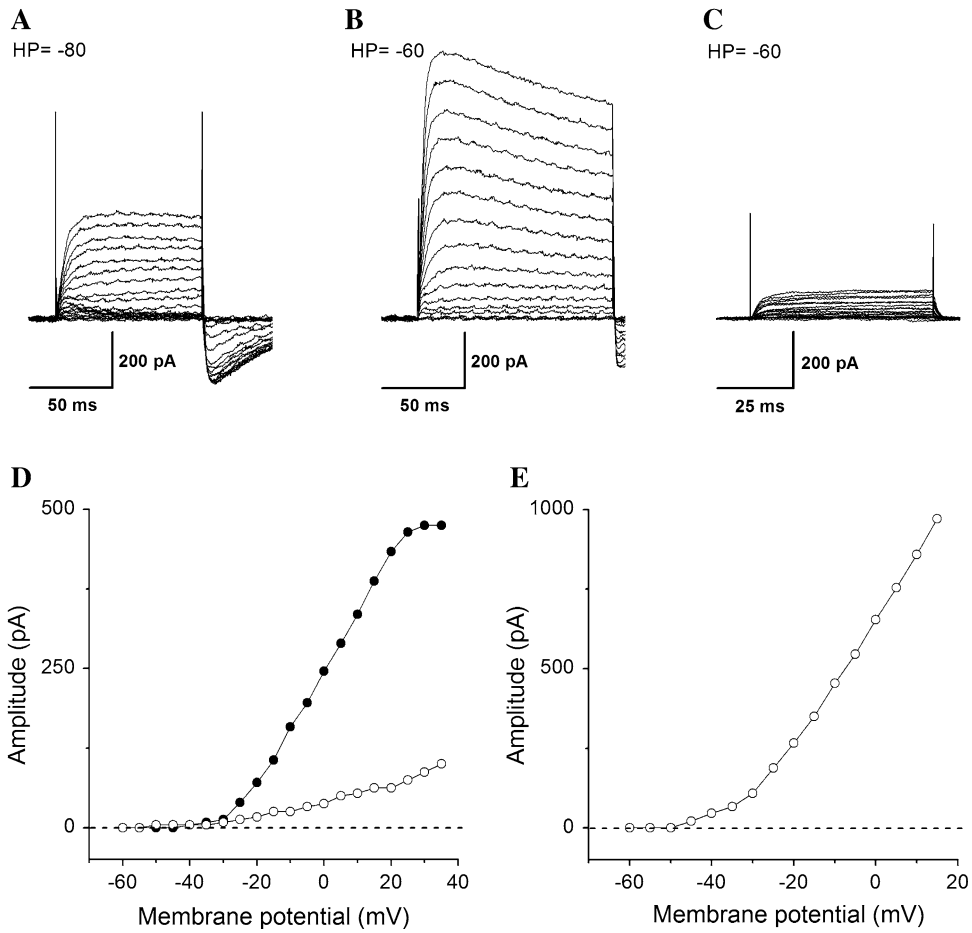

Fig. 5 Outward currents recorded from PC neurons. **a** A family of non-inactivating outward currents was elicited in response to depolarizing voltage steps from an HP of –80 to +20 mV (5 mV increments). **b** A family of outward currents with both transient and sustained components was elicited in response to depolarizing voltage steps between –80 and +20 mV (5-mV increments). **c** The delayed outward I_K was substantially attenuated in the presence of 50 mM TEA. **d** The *I–V* characteristics of the transient and delayed I_K revealed different activation thresholds and amplitudes

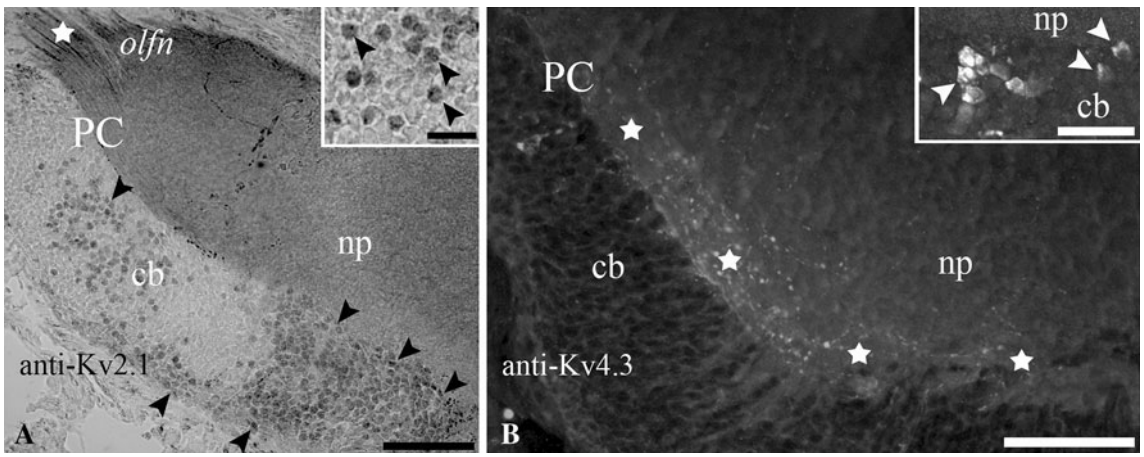

Fig. 6 Distribution of K-channel containing neurons in the PC. **a** An overview of the PC, displaying a large number of $K_V2.1$ immunoreactive cells (*arrowheads*) in the cb layer and an overall labeling in the np region. *Inset* higher magnification of labeled globuli cells (*arrowheads*). HRP-DAB reaction. **b**: Immunoreactivity in the PC, showing a bundle of varicose fibers (*stars*) running near the borderline between the cb and np layers. *Insert* a small group of $K_V4.3$ immunolabeled neurons (*arrowheads*) located between the cb and np layers. Immunofluorescence method, FITC labeling. *PC* procerebrum, *cb* cell body, *np* neuropile, *olfn* olfactory nerve. *Scale bars* **a**, **b** 50 μm; **a**, **b** *insert* 20 μm

fast I_{NaT} and a low-threshold I_{NaP} and the expression of $Na_V1.8$-like channels correlated with the presence of a slow I_{NaT} and I_{NaP}. We suggest that these cells correspond to bursting and non-bursting neurons, respectively. Our conclusion is supported by the IHC data, because $Na_V1.9$ and $Na_V1.8$ Abs specifically labeled morphologically

different types of PC neurons. The specificity of the Abs used was further verified by identification of the $Na_V\beta2$ subunit, which is expressed specifically in sensory neurons; the $Na_V\beta2$ Ab equally labeled both morphological types of neurons. In vertebrates, both the $Na_V1.9$ and $Na_V1.8$ channels contribute significantly to establish the membrane properties of primary afferent neurons and may be implicated in the molecular mechanisms of sensory cells (Renganathan et al. 2001). I_{NaP} is generally associated with setting the RMP and modulation of intrinsic high-frequency oscillations of neurons (Lipowsky et al. 1996; Parri and Crunelli 1998; Stuart and Sakmann 1995). Recently, however, it was found that I_{NaP} can also regulate the resting properties of the synapse and boost the effectiveness of presynaptic modulators (Huang and Trussell 2008).

The RMP, the rapid repolarization of the AP, and the spike frequency of excitable cells are primarily mediated by ion channels conducting K^+-ions. The outward I_K recorded from most PC cells fits well into the class of delayed rectifier K-channels responsible for rapid repolarization and for determining the RMP (Rudy 1988). Our IHC findings support the data obtained by these electrophysiological experiments, because a large number of neurons and the whole neuropil of the PC were labeled by $K_V2.1$ antibody. The presence of $K_V4.3$-like channels was demonstrated in a limited number of neurons located in small clusters near the neuropil layer of the PC. However, $K_V4.3$ Ab immunoreactive fibers were present in the terminal neuropil, suggesting that $K_V4.3$ channels are involved in modulating the integrated odor signals at the synaptic level. These channels play a physiological role in lowering firing frequency and modulating the efficacy of synaptic transmission (Rogawski 1985). It seems that the total outward current we observed in PC neurons has several components, including the delayed outward current, the inactivating or transient I_K, and presumably the Ca^{2+}-activated outward current.

The origin of the bursting activity

Although both spontaneous and odor-evoked bursting activities have been extensively studied, the origin of the bursting activity is still unknown. Contrary to observation made in *Limax*, the isolated PC cells of *Helix* did not show spontaneous activity. Bursting activity can, however, be initiated after re-establishing synaptic contacts between neurons in cell culture (Rhines et al. 1993b). Moreover, in *Limax*, the non-bursting cells fire APs, while the *Helix* cells studied here produce a bursting activity when recorded in situ using perforated patch-clamp (Watanabe et al. 1998). Here, we suggest that the neurons of the snail PC can be divided into two groups based on the expression of distinct voltage-gated ion channels, namely cells with bursting or non-bursting properties. The expression of ion-channel isoforms is likely to reflect functional specializations. The function of the laterally interconnected network of inhibitory bursting neurons is to ensure the resting oscillation and synchronous activity of several of these cells. Our electrophysiological data suggested that $Na_V1.9$ is responsible for the resting oscillatory activity and $Na_V1.8$ for the stimulus-evoked activity of the PC cells. Whether the oscillatory activity is completely intrinsic to the bursting neurons of the *Helix* PC, or is at least partly of extrinsic origin, is unknown. It was described that the background activity of the PC is limited to the cell body layer whereas the odor-evoked activity was observed in the neuropil (Nikitin and Balaban 2000). Ito et al. (2004) have observed that neurons in the digits and TG both contribute to the spontaneous activity recorded from the tentacular nerve of *Limax*; therefore, the oscillatory activity observed in the *Helix* PC could be determined by the activity of the digits and TG as well as by intrinsic membrane properties of the PC neurons.

Acknowledgments This work was supported by the Hungarian Scientific Research Fund No. 78224.

References

Ache BW, Young JM (2005) Olfaction: diverse species, conserved principles. Neuron 48:417–430

Azanza MJ, Pérez-Castejón C, Pes N, Pérez-Bruzón RN, Aisa J, Junquera C, Maestú C, Lahoz M, Martínez-Ciriano C, Vera-Gil A, del Moral A (2008) Characterization by immunocytochemistry of ionic channels in *Helix aspersa* suboesophageal brain ganglia neurons. Histol Histopathol 23:397–406

Balaban PM, Maksimova OA (1993) Positive and negative brain zones in the snail. Eur J Neurosci 5:768–774

Battonyai I, Elekes K (2012) The 5-HT immunoreactive innervation of the *Helix* procerebrum. Acta Biol Hung 63:96–103

Bullock TH, Horridge GA (1965) Structure and function in the nervous system of invertebrates. Freeman and Co, San Francisco

Chase R (2000) Structure and function in the cerebral ganglion. Microsc Res Tech 49:511–520

Chase R (2002) Behavior and its neural control in gastropod mollusks. Oxford University Press, Oxford

Chase R, Tolloczko B (1993) Tracing neural pathways in snail olfaction: from the tip of the tentacles to the brain and beyond. Microsc Res Tech 24:214–230

Chen N, Lucero MT (1999) Transient and persistent tetrodotoxin-sensitive sodium currents in squid olfactory receptor neurons. Journal of comparative physiology a-sensory neural and behavioral physiology 184:63–72

Cooke IR, Gelperin A (1988) Distribution of FMRFamide-like immunoreactivity in the nervous system of the slug *Limax maximus*. Cell Tissue Res 253:69–76

Delaney KR, Gelperin A, Fee MS, Flores J, Gervais R, Tank DW, Kleinfeld D (1994) Waves and stimulus-modulated dynamics in an oscillating olfactory network. Proc Nat Acad Sci USA 91:669–673

Elekes K, Nassel DR (1990) Distribution of FMRFamide-like immunoreactive neurons in the central-nervous-system of the snail *Helix pomatia*. Cell Tissue Res 262:177–190

Elekes K, Battonyai I, Kobayashi S, Ito E (2012) Organization of the procerebrum in terrestrial pulmonates (*Helix, Limax*) reconsidered: Cell mass layer synaptology and its serotonergic input system. Brain Structure Function. doi:10.1007/s00429-012-0409-2

Ermentrout B, Flores J, Gelperin A (1998) Minimal model of oscillations and waves in the *Limax* olfactory lobe with tests of the model's predictive power. J Neurophysiol 79:2677–2689

Gelperin A (1999) Oscillatory dynamics and information processing in olfactory systems. J Exp Biol 202:1855–1864

Gelperin A, Tank DW (1990) Odour-modulated collective network oscillations of olfactory interneurons in a terrestrial mollusc. Nature 345:437–440

Gelperin LD, Rhines D, Flores J, Tank DW (1993) Coherent network oscillations by olfactory interneurons: modulation by endogenous amines. J Neurophysiol 69:1930–1939

Gelperin A, Flores J, Raccuia-Behling F, Cooke IRC (2000) Nitric oxide and carbon monoxide modulate oscillations of olfactory interneurons in a terrestrial mollusk. J Neurophysiol 83:116–127

Gervais R, Kleinfeld D, Delaney KR, Gelperin A (1996) Central and reflex neuronal response elicited by odor in a terrestrial mollusk. J Neurophysiol 76:1327–1339

Gilly WF, Gillette R, McFarlane M (1997) Fast and slow activation kinetics of voltage-gated sodium channels in molluscan neurons. J Neurophysiol 77:2373–2384

Hernadi L, Terano Y, Muneoka Y, Kiss T (1995) Distribution of catch-relaxing peptide (CARP)-like immunoreactive neurons in the central and peripheral nervous system of *Helix pomatia*. Cell Tissue Res 280:335–348

Hildebrand JG, Shepherd GM (1997) Mechanisms of olfactory discrimination: converging evidence for common principles across phyla. Annu Rev Neurosci 20:595–631

Huang H, Trussell LO (2008) Control of presynaptic function by a persistent Na^+ current. Neuron 60:975–979

Inoue T, Watanabe S, Kirino Y (2001) Serotonin and NO complementarily regulate generation of oscillatory activity in the olfactory CNS of a terrestrial mollusk. J Neurophysiol 85: 2634–2638

Ito I, Kimura T, Watanabe S, Kirino Y, Ito E (2004) Modulation of two oscillatory networks in the peripheral olfactory system by γ-aminobutyric acid, glutamate, and acetylcholine in the terrestrial slug *Limax marginatus*. J Neurobiol 59:304–318

Kimura T, Toda S, Sekiguchi T, Kirino Y (1998) Behavioral modulation induced by food odor aversion conditioning and its influence on the olfactory responses of an oscillatory brain network in the slug, *Limax marginatus*. Learn Mem 4:365–375

Kiss T, László Z, Pirger Z (2012) Cellular localization and kinetic properties of $Na_v1.9$-, $Na_v1.8$-, and $Na_v1.7$-like channel subtypes in *Helix pomatia*. Neuroscience 203:78–90

Kleinfeld D, Delaney KR, Fee MS, Flores JA, Tank DW, Gelperin A (1994) Dynamics of propagating waves in the olfactory network of a terrestrial mollusk: an electrical and optical study. J Neurophysiol 72:1402–1419

Kobayashi S, Hattori M, Elekes K, Ito E, Matsuo R (2010) FMRFamide regulates oscillatory activity of the olfactory center in the slug. Eur J Neurosci 32:1180–1192

Lipowsky R, Gillessen T, Alzheimer C (1996) Na^+ channels amplify EPSPs in hippocampal ca1 pyramidal cells. J Neurophysiol 76:2181–2191

Llinas RR (1988) The intrinsic electrophysiological properties of mammalian neurons: insights into central nervous system function. Science 242:1654–1664

Nikitin ES, Balaban PM (2000) Optical recording of odor-evoked responses in the olfactory brain of the naive and aversively trained terrestrial snails. Learn Mem 7:422–432

Nikitin ES, Zakharov IS, Samarova EI, Kemenes G, Balaban PM (2005) Fine tuning of olfactory orientation behaviour by the interaction of oscillatory and single neuronal activity. Eur J Neurosci 22:2833–2844

Parri HR, Crunelli V (1998) Sodium current in rat and cat thalamocortical neurons: role of a non-inactivating component in tonic and burst firing. J Neurosci 18:854–867

Ratte S, Chase R (1997) Morphology of interneurons in the procerebrum of the snail *Helix aspersa*. J Comp Neur 384:359–372

Ratté S, Chase R (2000) Synapse distribution of olfactory interneurons in the procerebrum of the snail *Helix aspersa*. J Comp Neurol 417:366–384

Renganathan M, Cummins TR, Waxman SG (2001) Contribution of Na_v 1.8 sodium channels to action potential electrogenesis in DRG neurons. J Neurophysiol 86:629–640

Rhines DL, Sokolove PG, Flores J, Tank DW, Gelperin A (1993a) Cultured olfactory interneurons from *Limax maximus*: optical and electrophysiological studies of transmitter-evoked responses. J Neurophysiol 69:1940–1947

Rhines LD, Sokolove PG, Flores J, Tank DW, Gelperin A (1993b) Cultured olfactory interneurons from *Limax maximus*: optical and electrophysiological studies of transmitter-evoked responses. J Neurophysiol 69:1940–1947

Rogawski MA (1985) The A-current: how ubiquitous a feature of excitable cells is it. Trends Neurosci 8:214–219

Rudy B (1988) Diversity and ubiquity of K channels. Neurosci 25:729–749

Schütt A, Bullock TH, Basar R (2000) Odor input generates ~1.5 hz and ~1.3 hz spectral peaks in the *Helix* pedal ganglion. Brain Res 879:73–87

Stuart G, Sakmann B (1995) Amplification os EPSPs by axosomatic sodium channels in neocortical pyramidal neurons. Neuron 15:1065–1076

Wang JW, Denk W, Flores J, Gelperin A (2001) Initiation and propagation of calcium-dependent action potentials in a coupled network of olfactory interneurons. J Neurophysiol 85:977–985

Watanabe S, Kawahara S, Kirino Y (1998) Morphological characterization of the bursting and nonbursting neurones in the olfactory centre of the terrestrial slug *Limax marginatus*. J Exp Biol 201:925–930

Zaitseva OV (2000) Structural organization of procerebrums of terrestrial molluscs:characteristics of neuronal pattern, plasticity, and age peculiarities. J Evol Biochem Physiol 36:246–253

Zs-Nagy I, Sakharov DA (1970) The fine structure of the procerebrum of pulmonate molluscs, *Helix* and *Limax*. Tissue and Cell 2:399–411